SUPPORTING INFORMATION- FIGURES

Layers stacking disorder in Mg-Fe chlorites based on powder X-ray diffraction data

Katarzyna Luberda-Durnaś[1], Marek Szczerba[1], Małgorzata Lempart[1], Zuzanna Ciesielska[1], Arkadiusz Derkowski[1]

[1]Institute of Geological Science, Polish Academy of Science, Senacka 1, 31-002 Krakow

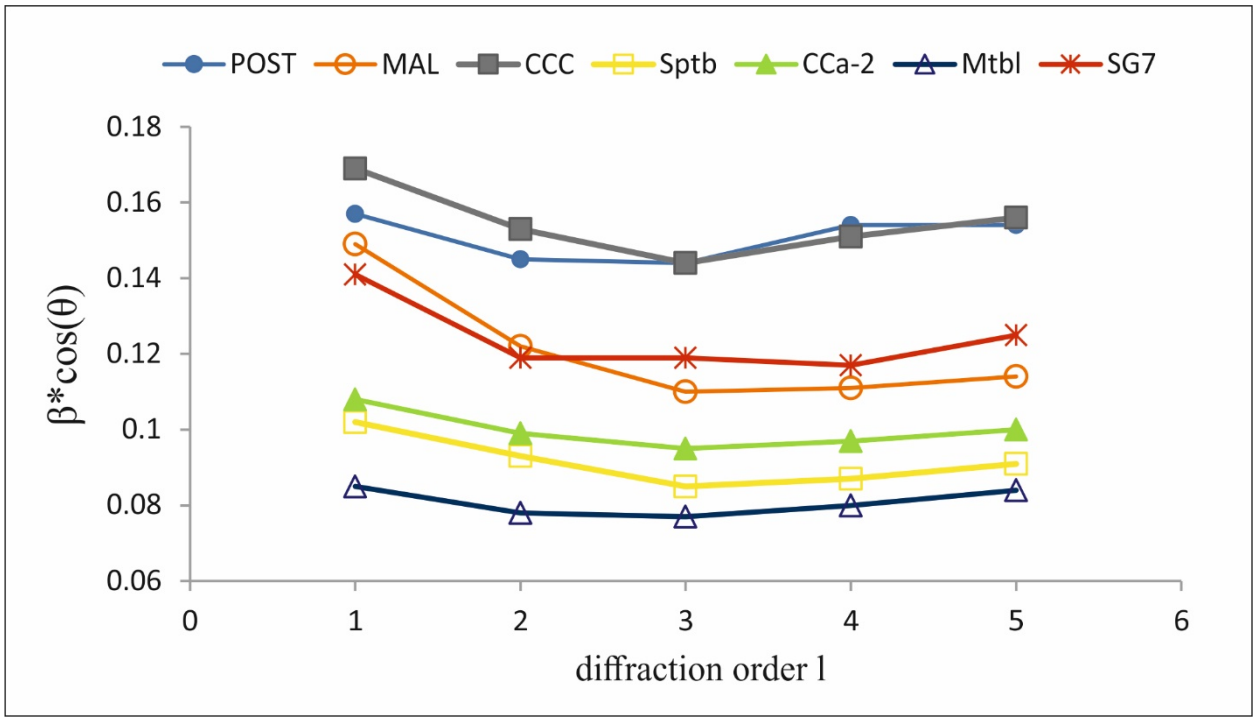

Figure SI 1. Calculated XRD peak breadths (with stripped $K_{\alpha 2}$) multiplied by cos(θ) for the investigated chlorites vs. *00l* diffraction order for the 001 to 005 reflections; disoriented powder specimens.

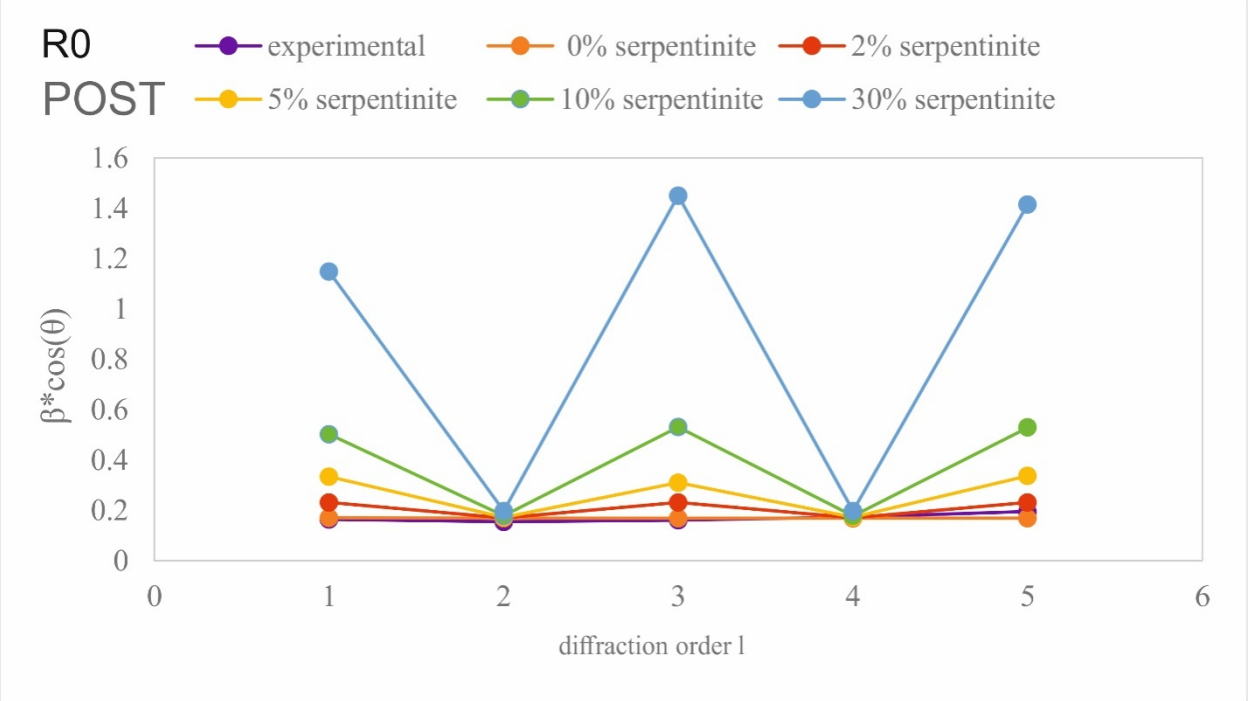

Figure SI 2. Calculated XRD peak breadths (with stripped $K_{\alpha 2}$) multiplied by cos(θ) for the investigated chlorite POST and simulated diffraction patterns for different serpentinite content vs. *00l* diffraction order for the 001 to 005 reflections.

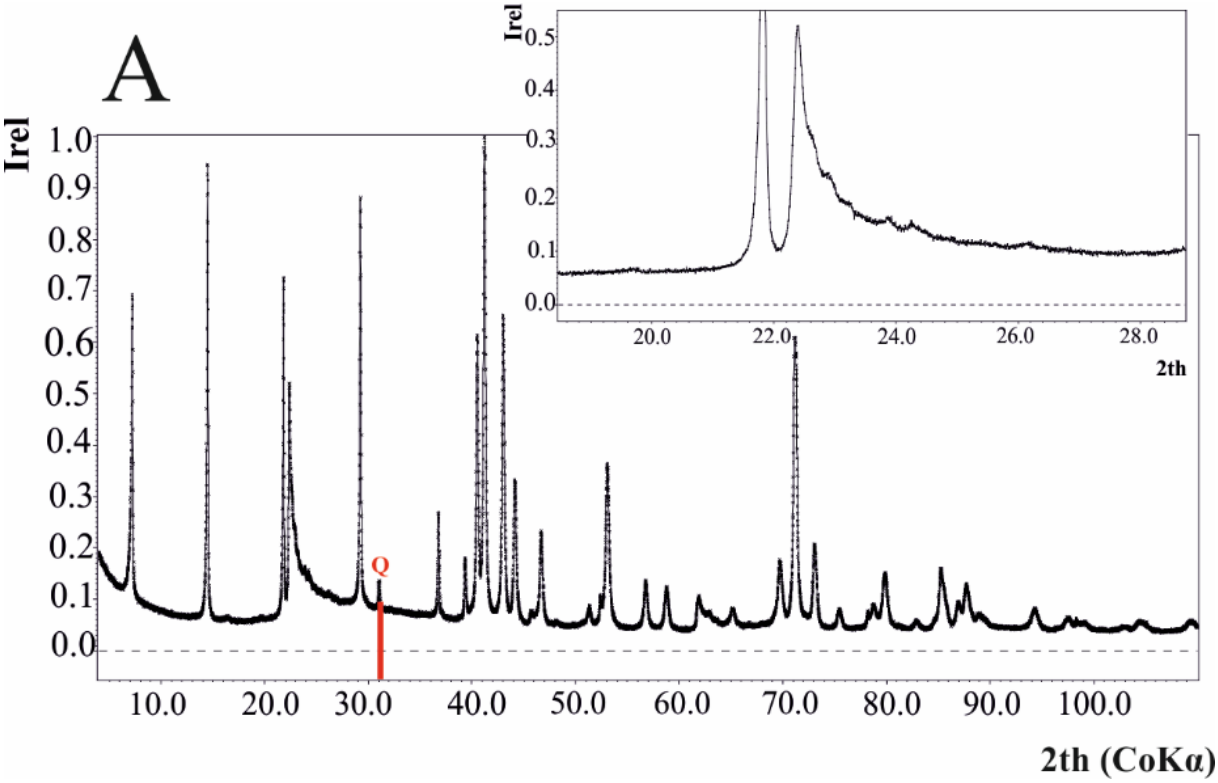
A
Irel
1.0
0.9
0.8
0.7
0.6
0.5
0.4
0.3
0.2
0.1
0.0
Q
10.0
20.0
30.0
40.0
50.0
60.0
70.0
80.0
90.0
100.0
2th (CoKα)
Irel
0.5
0.4
0.3
0.2
0.1
0.0
20.0
22.0
24.0
26.0
28.0
2th

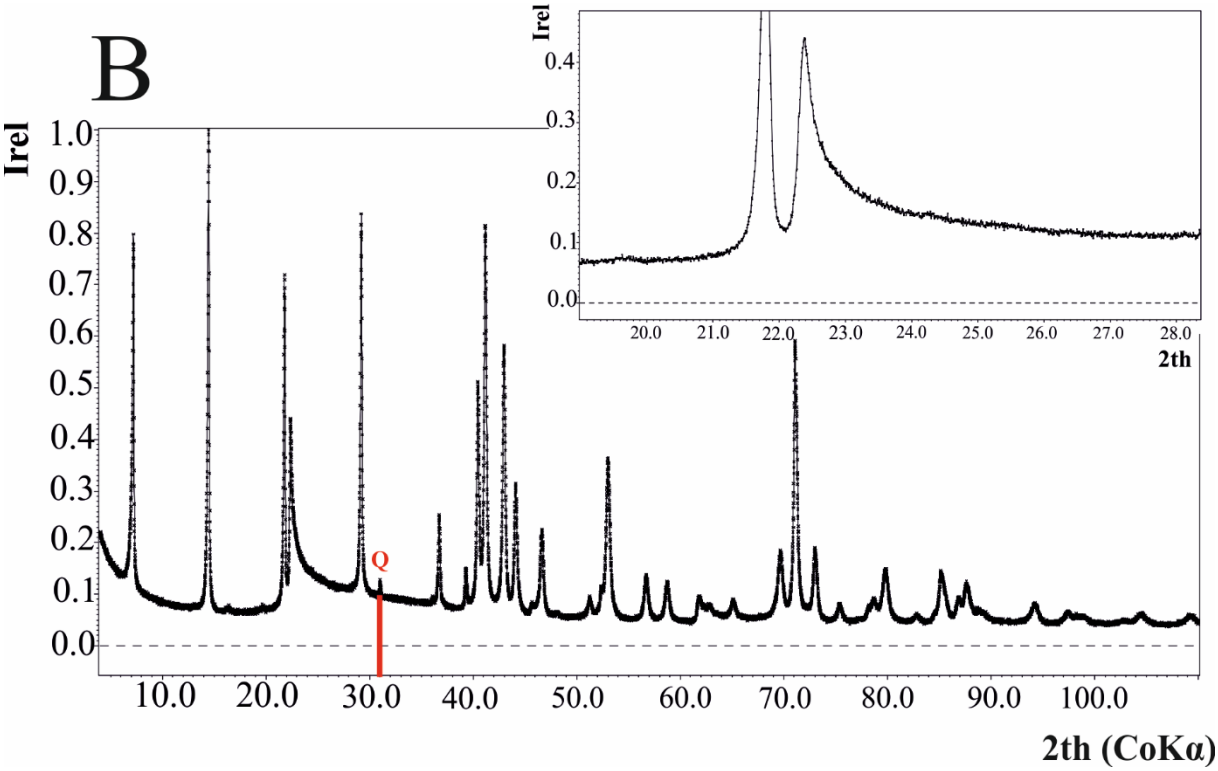
B
Irel
1.0
0.9
0.8
0.7
0.6
0.5
0.4
0.3
0.2
0.1
0.0
Q
10.0
20.0
30.0
40.0
50.0
60.0
70.0
80.0
90.0
100.0
2th (CoKα)
Irel
0.4
0.3
0.2
0.1
0.0
20.0
21.0
22.0
23.0
24.0
25.0
26.0
27.0
28.0
2th

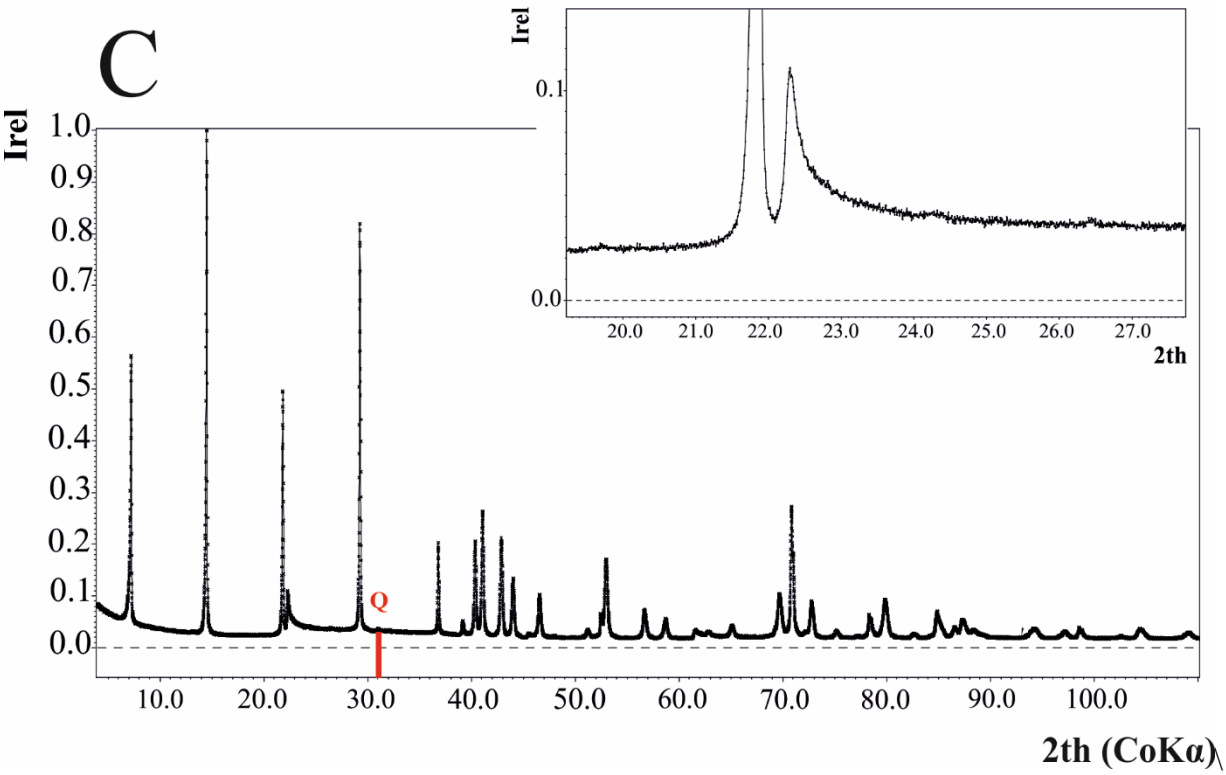
C
Irel
1.0
0.9
0.8
0.7
0.6
0.5
0.4
0.3
0.2
0.1
0.0
Q
10.0
20.0
30.0
40.0
50.0
60.0
70.0
80.0
90.0
100.0
2th (CoKα)
Irel
0.1
0.0
20.0
21.0
22.0
23.0
24.0
25.0
26.0
27.0
2th

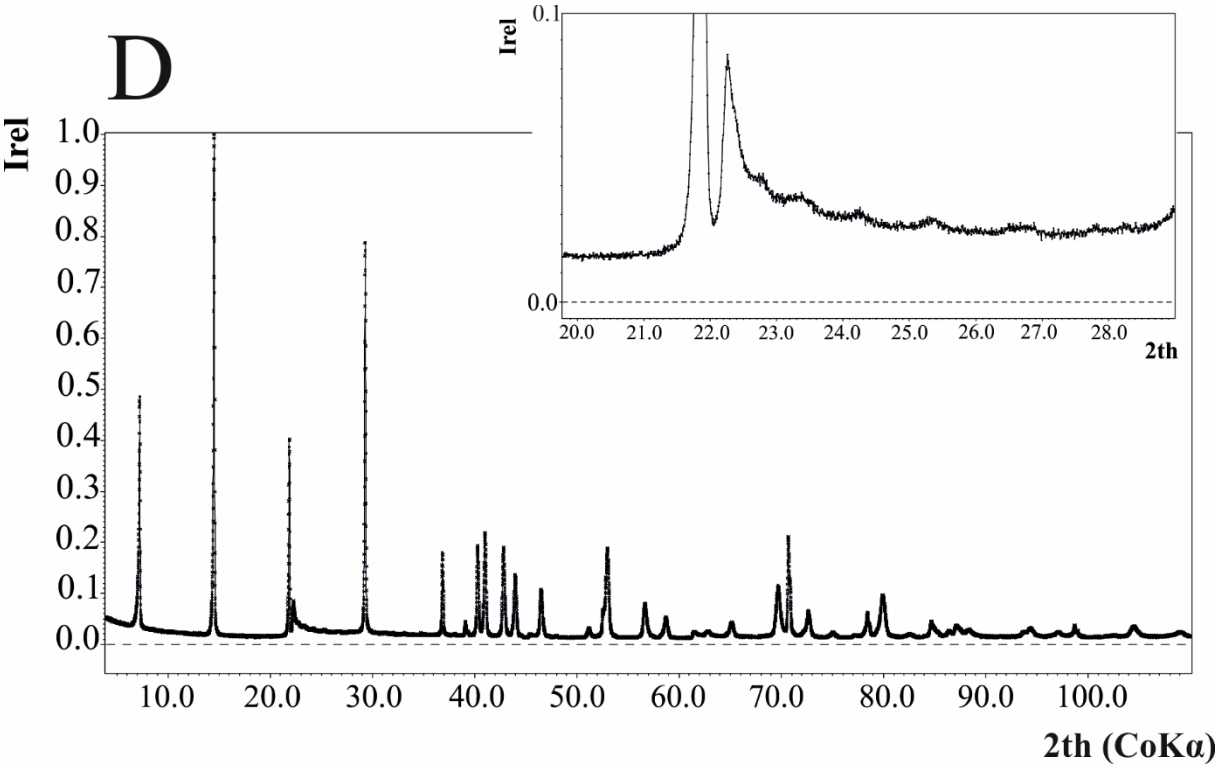
D
Irel
1.0
0.9
0.8
0.7
0.6
0.5
0.4
0.3
0.2
0.1
0.0
10.0
20.0
30.0
40.0
50.0
60.0
70.0
80.0
90.0
100.0
2th (CoKα)
Irel
0.1
0.0
20.0
21.0
22.0
23.0
24.0
25.0
26.0
27.0
28.0
2th

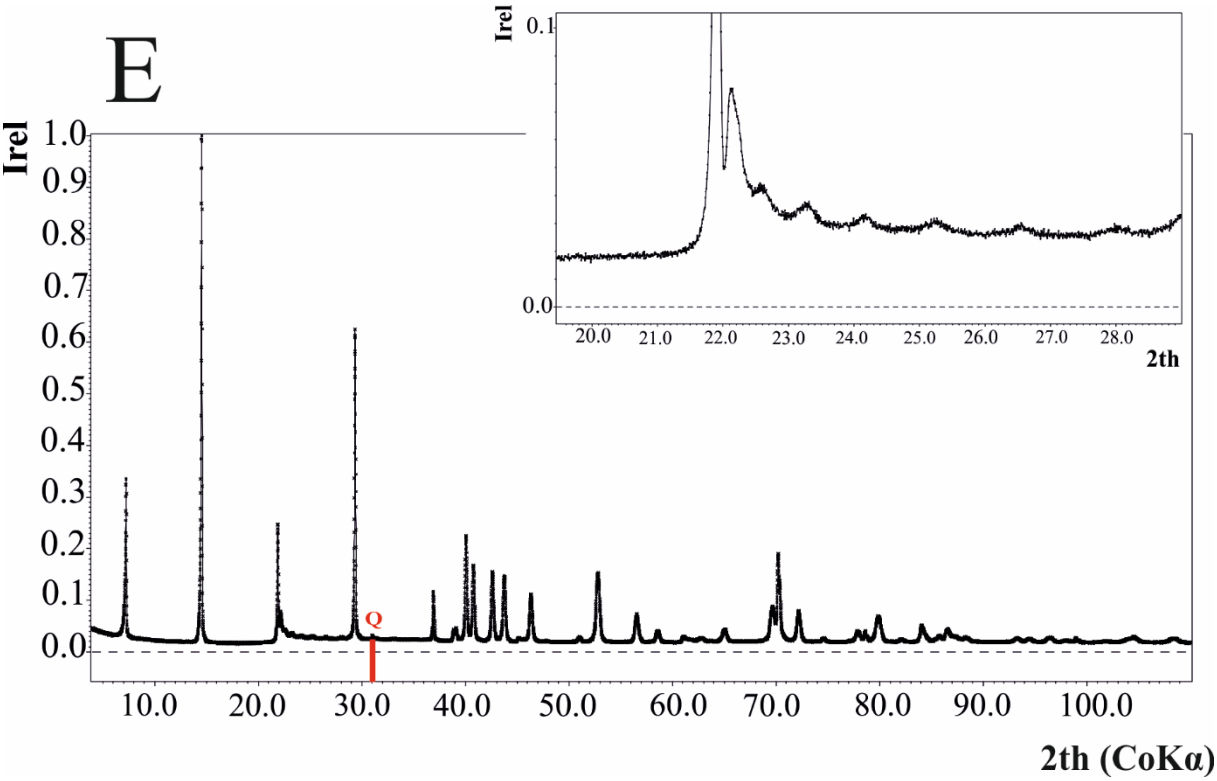

Figure SI 3. XRD patterns for chlorites (**a**) MAL (**b**) CCC (**c**) Sptb (**d**) CCa-2 (**e**) Mtbl; capillary measurement (2r=3mm). The most intense peaks of admixtures are pointed out by red lines (R-rutile, Q-quartz).

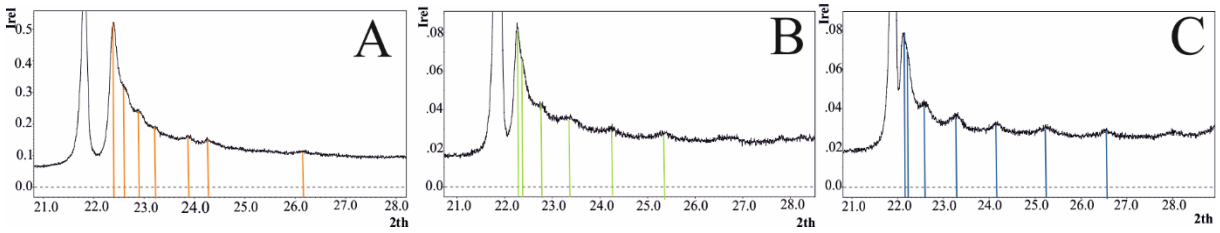

Figure SI 4. XRD patterns in the range 20-28° 2θ (CoKα) with marked reflections used for indexing: (**a**) MAL, (**b**) CCa-2, (**c**) Mtbl.

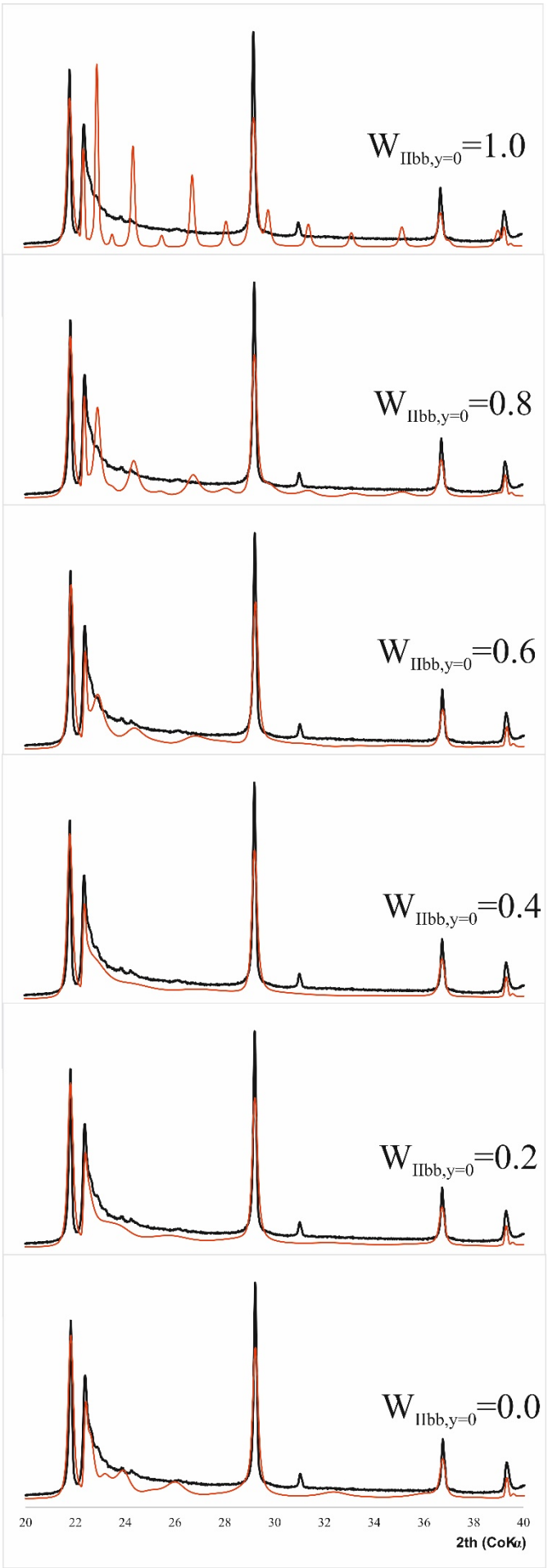

Figure SI 5. Comparison of experimental (black) and simulated (red) XRD patterns of the semi-random stacking structure of **chlorite MAL** in the range 20-40 °2θ for different values of $W_{IIbb,y=0}$**b**.

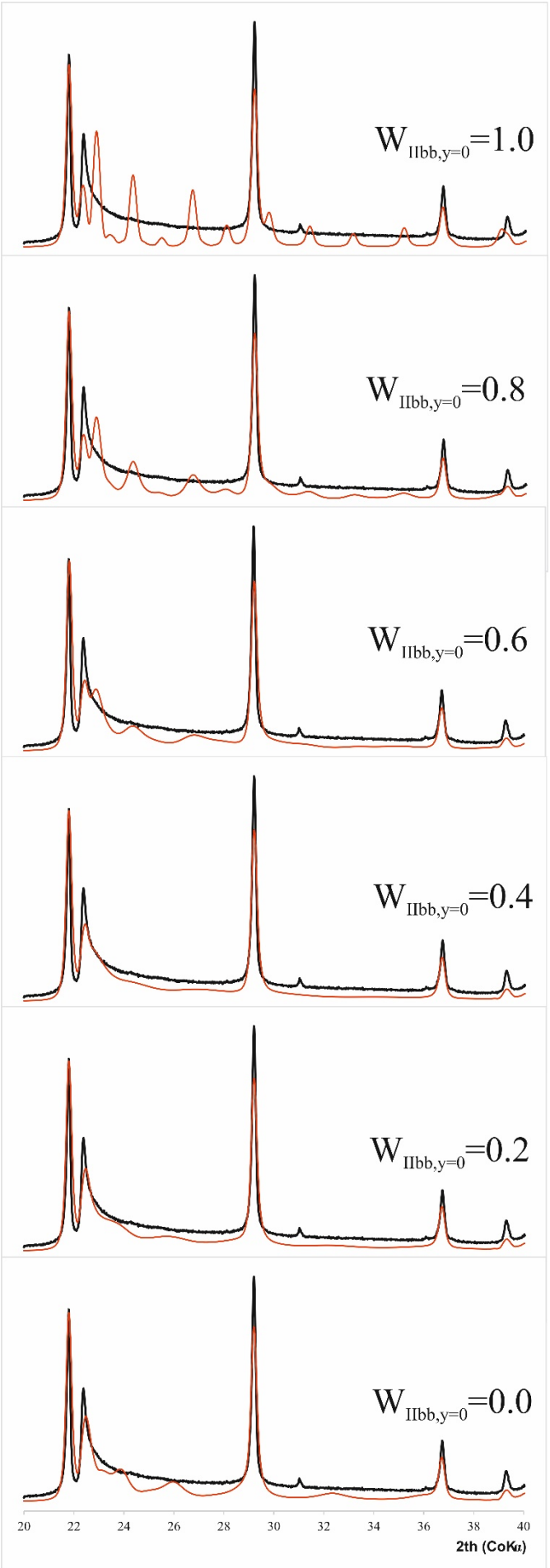

Figure SI 6. Comparison of experimental (black) and simulated (red) XRD patterns of semi-random stacking structure of **chlorite CCC** in the range 20-40 °2θ for different values of $W_{IIbb,y=0}$.

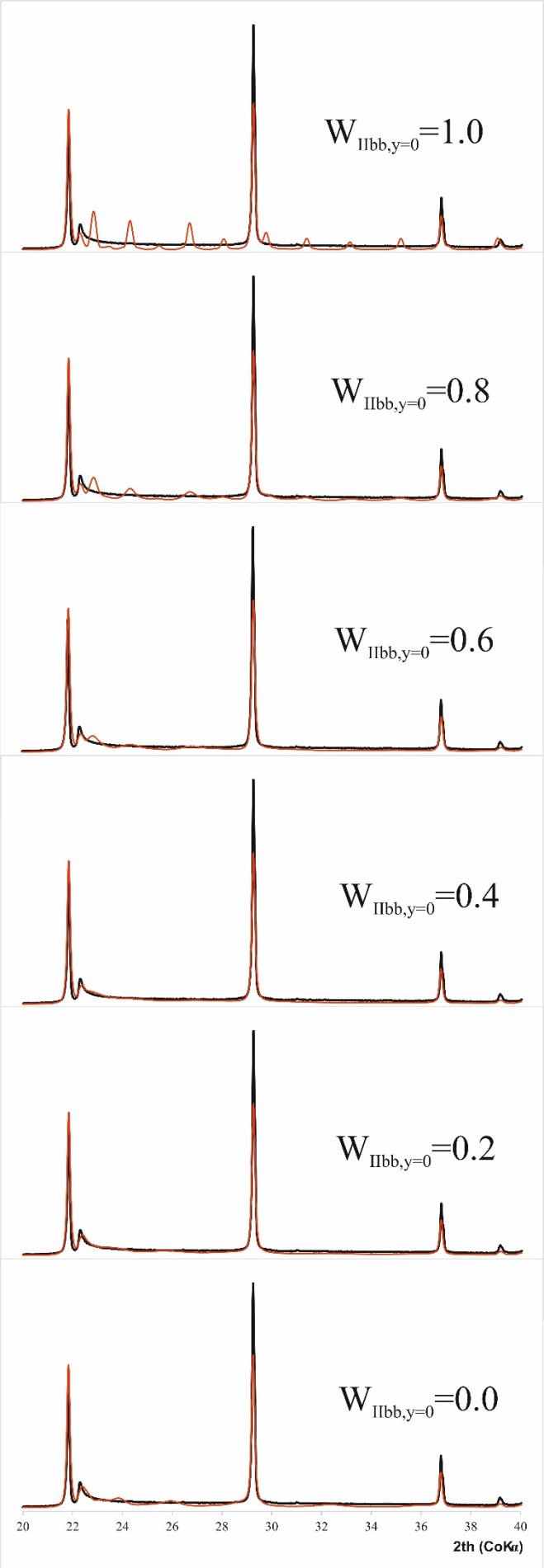

Figure SI 7. Comparison of experimental (black) and simulated (red) XRD patterns of semi-random stacking **chlorite Sptb** in the range 20-40 °2θ for different values of $W_{IIbb,y=0}$**b**.

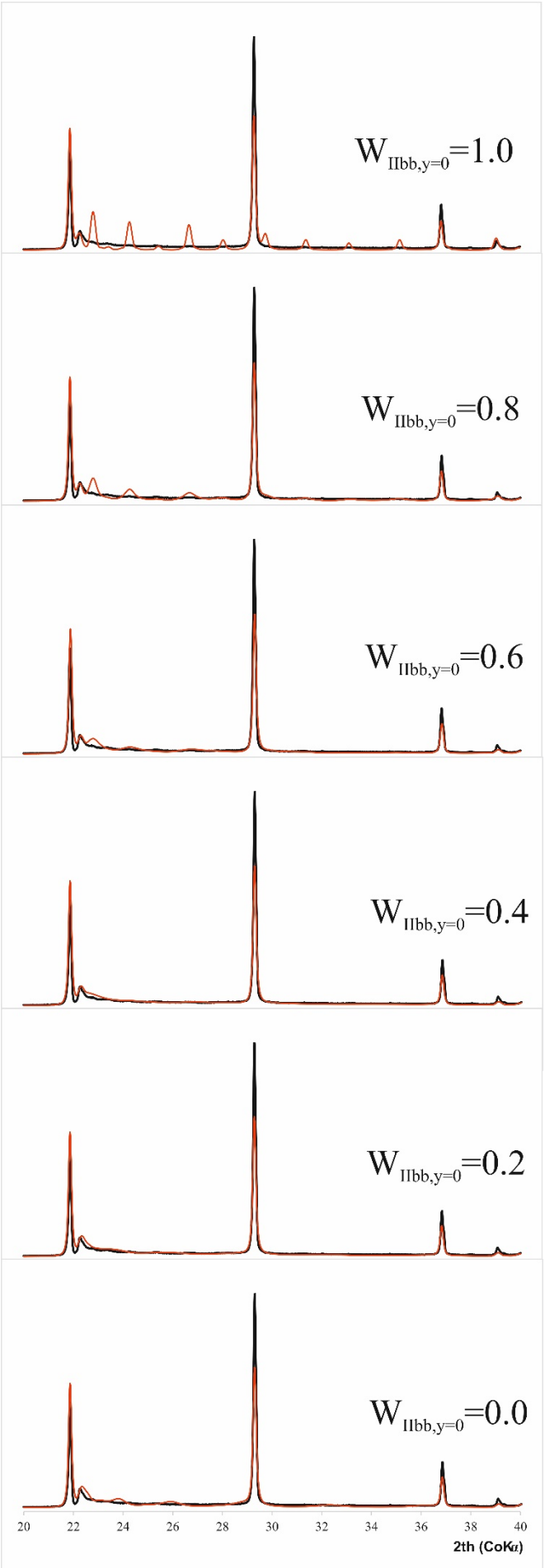

Figure SI 8. Comparison of experimental (black) and simulated (red) XRD patterns of semi-random stacking **chlorite CCa-2** in the range 20-40 °2θ for different values of $W_{IIbb,y=0}$**b**.

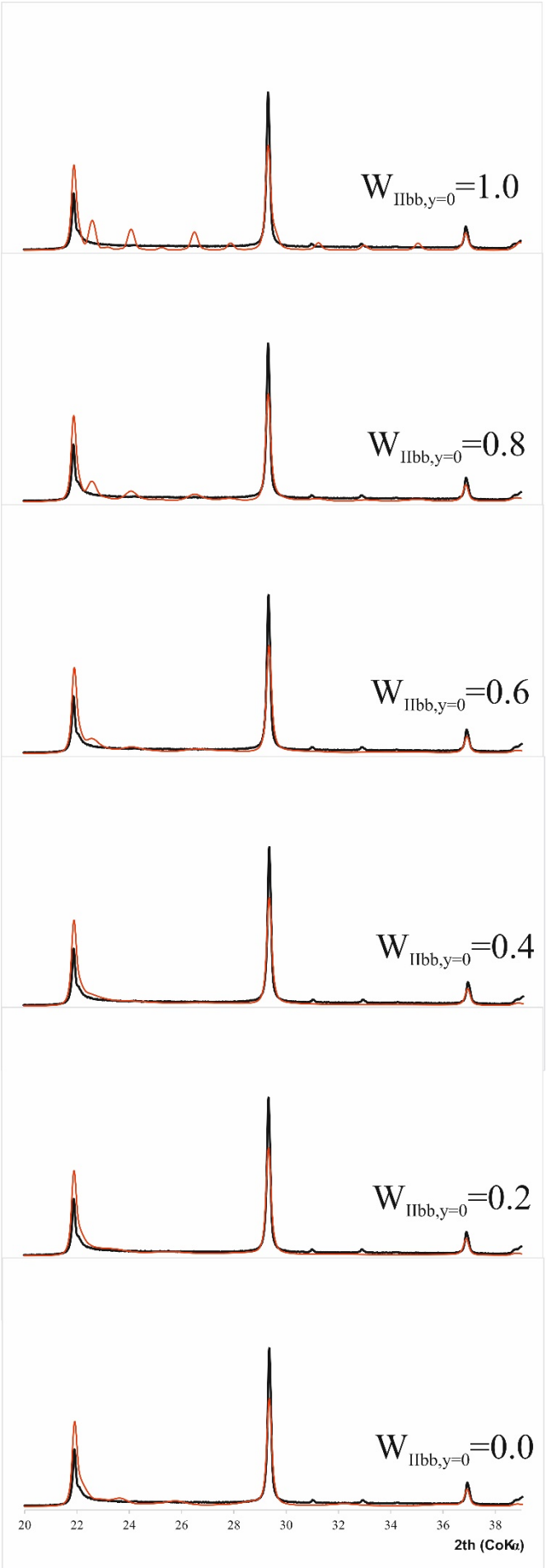

Figure SI 9. Comparison of experimental (black) and simulated (red) XRD patterns of semi-random stacking **chlorite SG7** in the range 20-40 °2θ for different values of $W_{IIbb,y=0}$**b**.

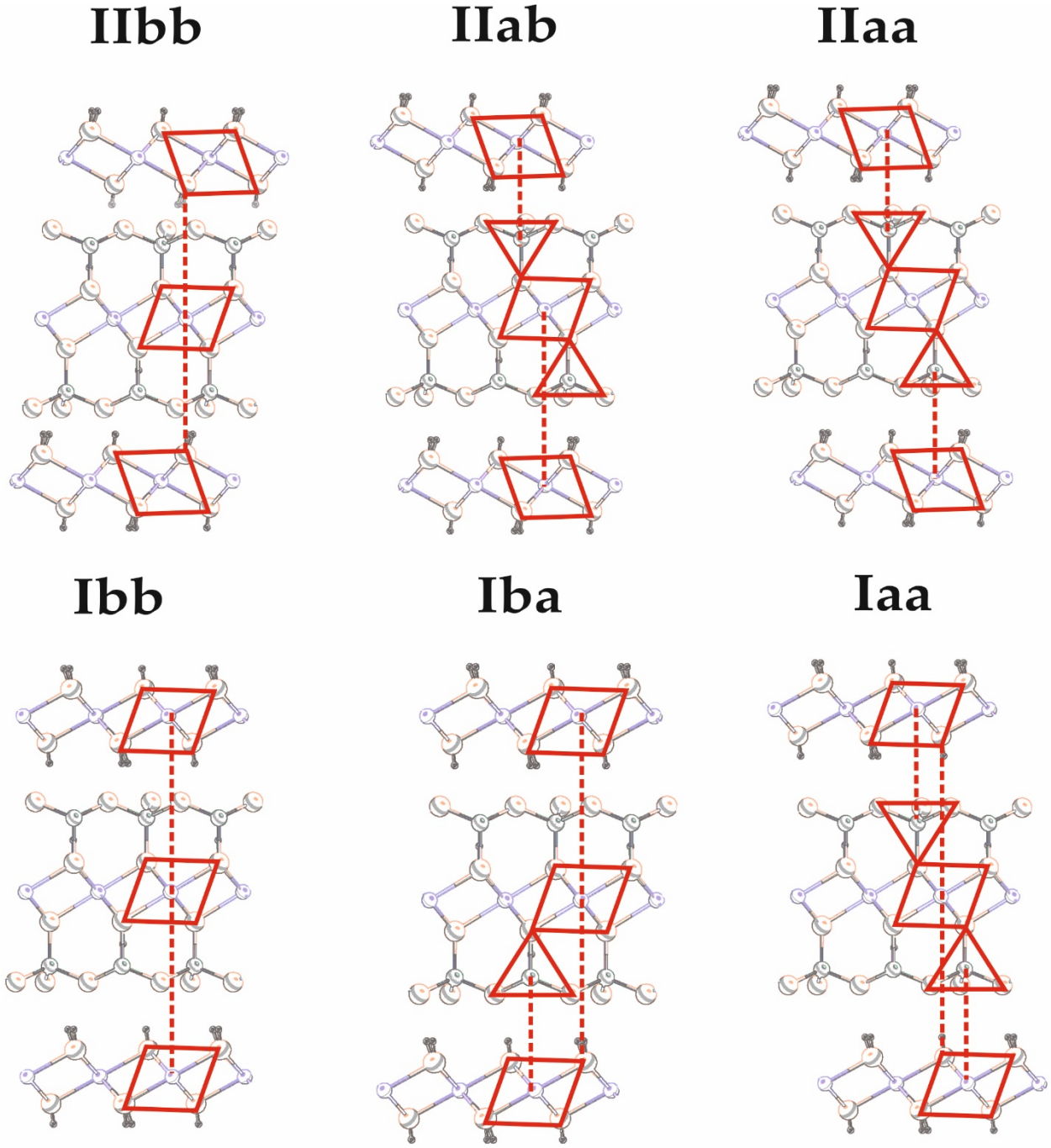

Figure SI 10. The differences between chlorite polytypes.

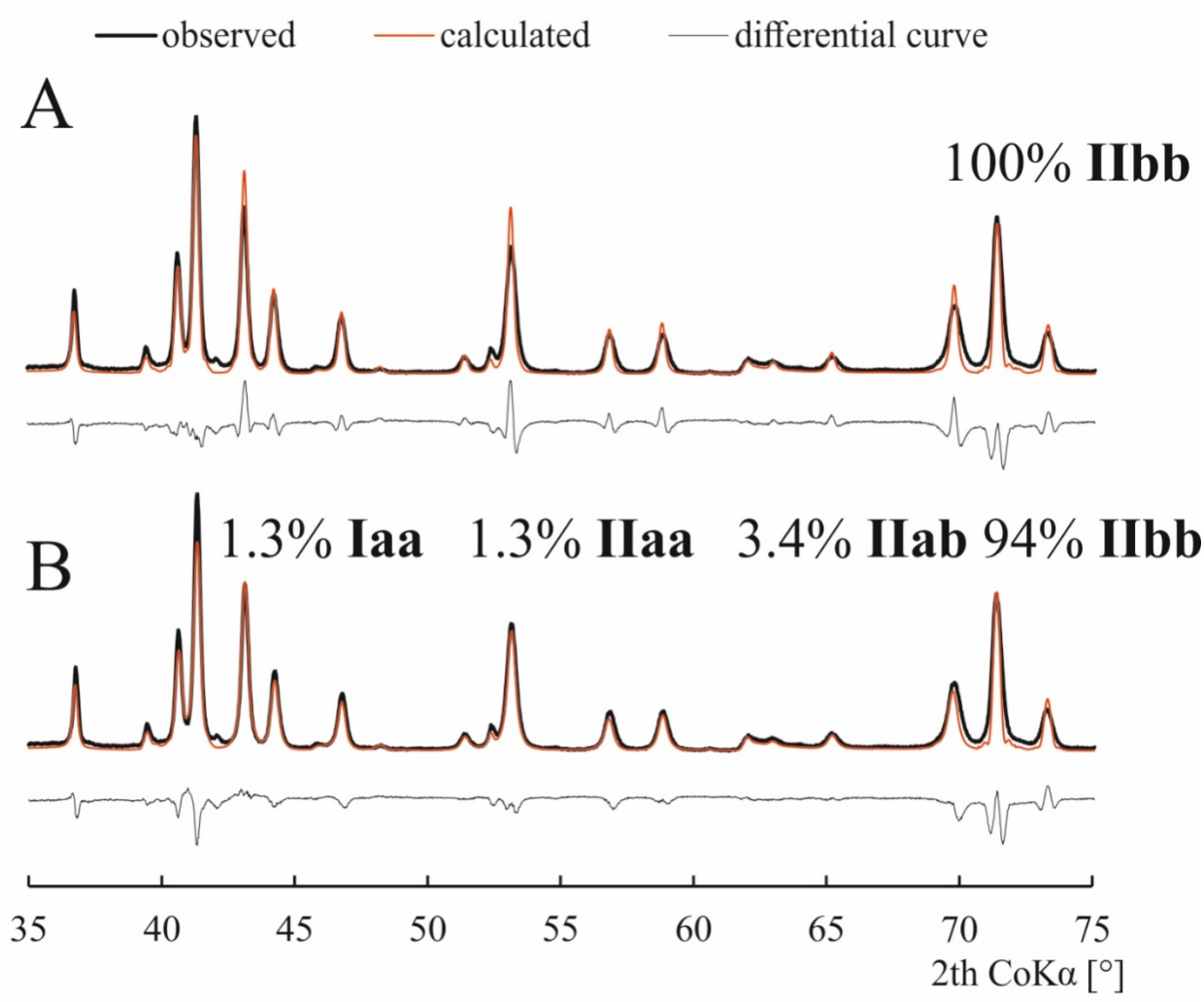

Figure SI 11. Comparison of experimental (black) and simulated (red) XRD patterns for POST chlorite **A)** without and **B)** with consideration of interstratification with polytypes other than IIbb.

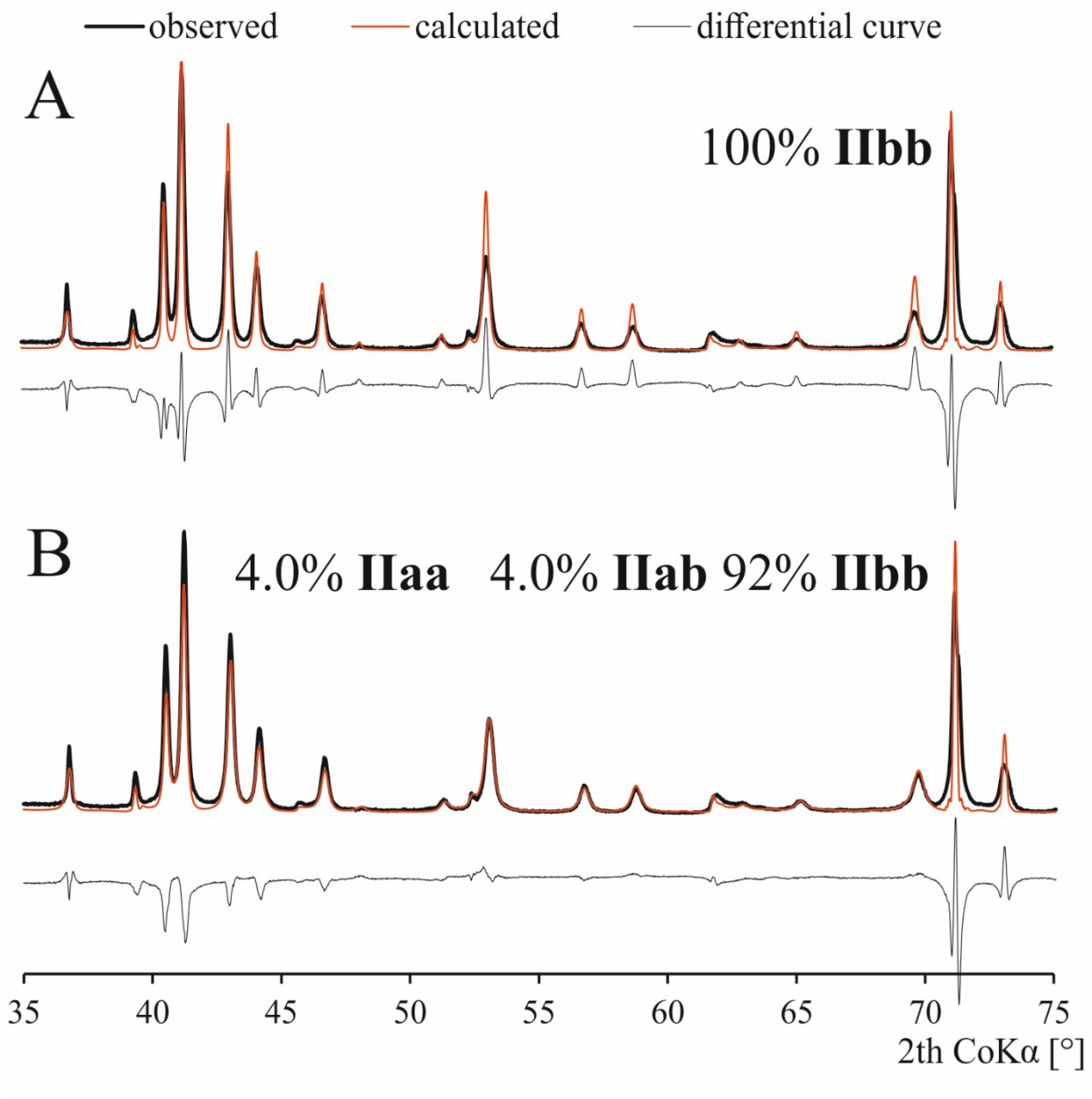

Figure SI 12. Comparison of experimental (black) and simulated (red) XRD patterns for MAL chlorite **A)** without and **B)** with consideration of interstratification with polytypes other than IIbb.

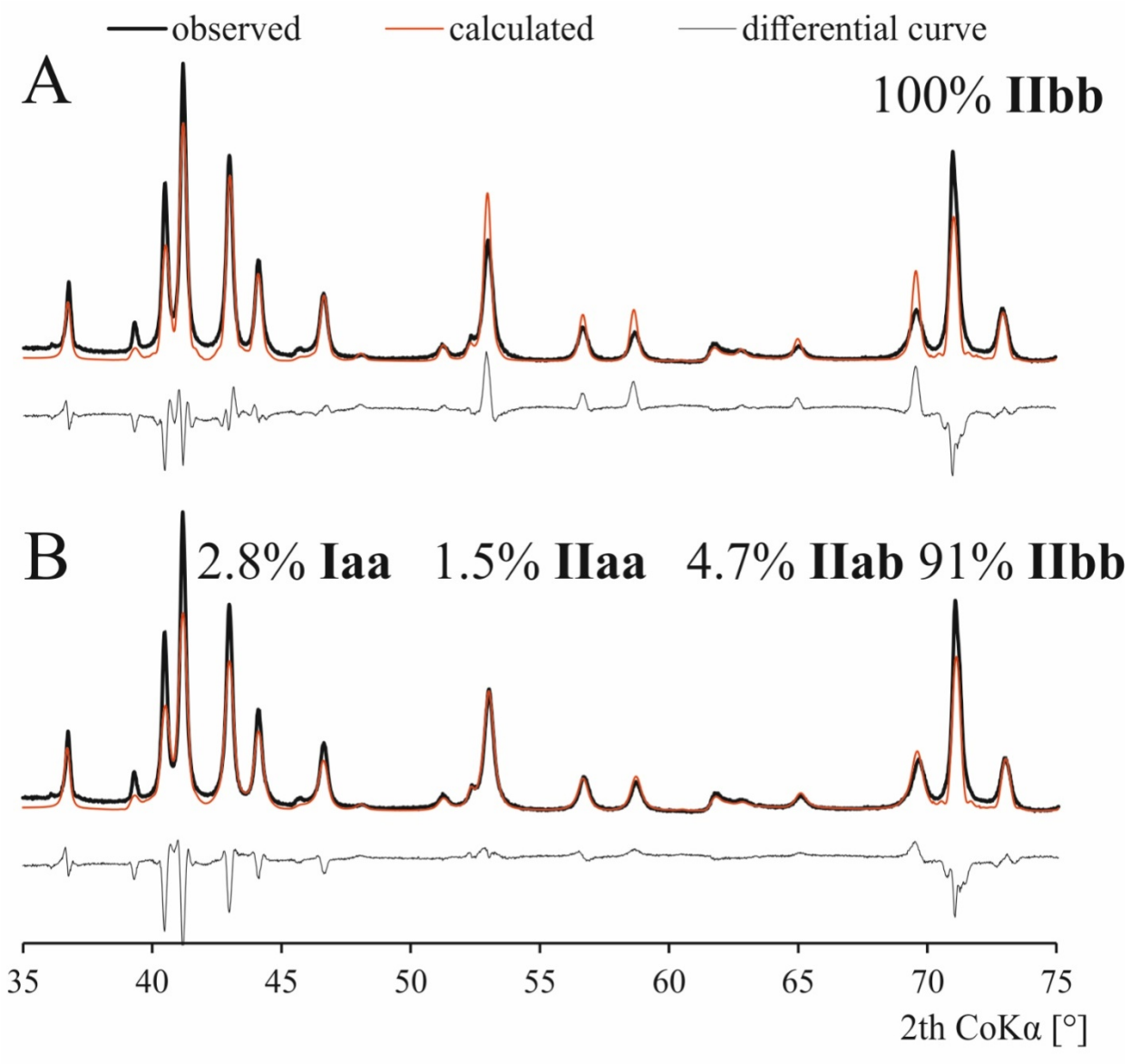

Figure SI 13. Comparison of experimental (black) and simulated (red) XRD patterns for CCC chlorite **A)** without and **B)** with consideration of interstratification with polytypes other than IIbb.

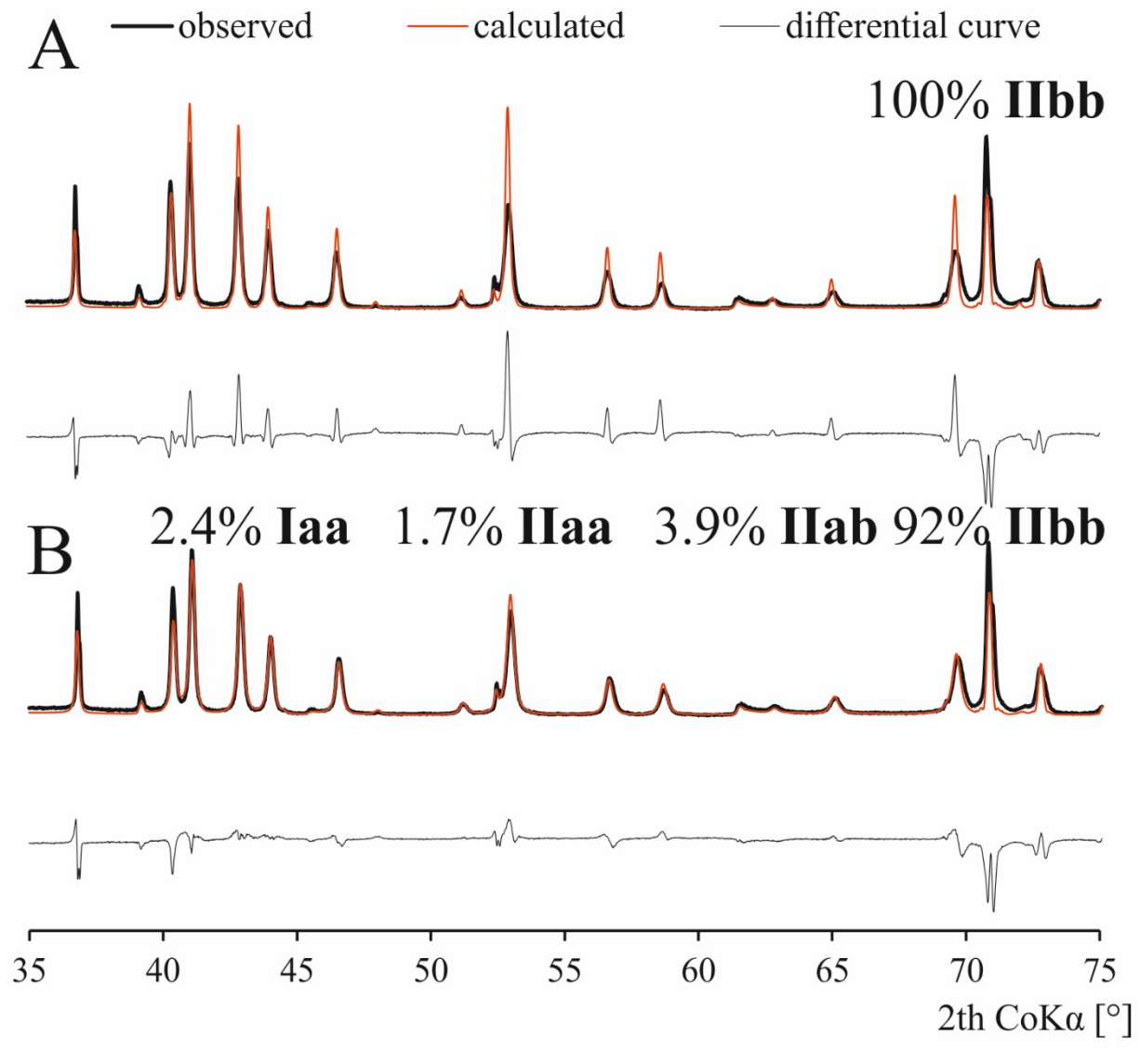

Figure SI 14. Comparison of experimental (black) and simulated (red) XRD patterns for Sptb chlorite **A)** without and **B)** with consideration of interstratification with polytypes other than IIbb.

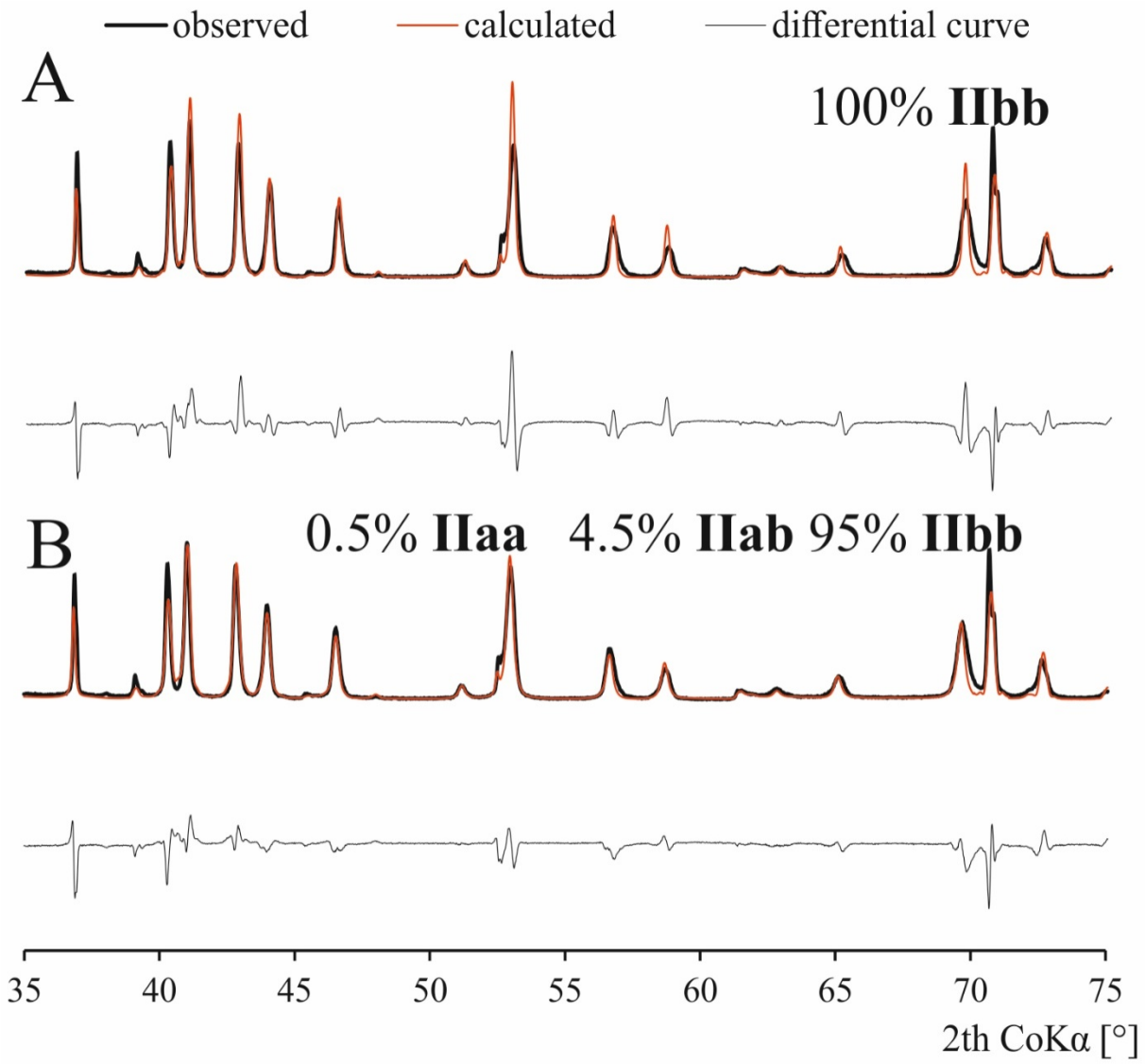

Figure SI 15 Comparison of fits for CCa-2 chlorite **A)** without and **B)** with consideration of interstratification with polytypes other than IIbb.

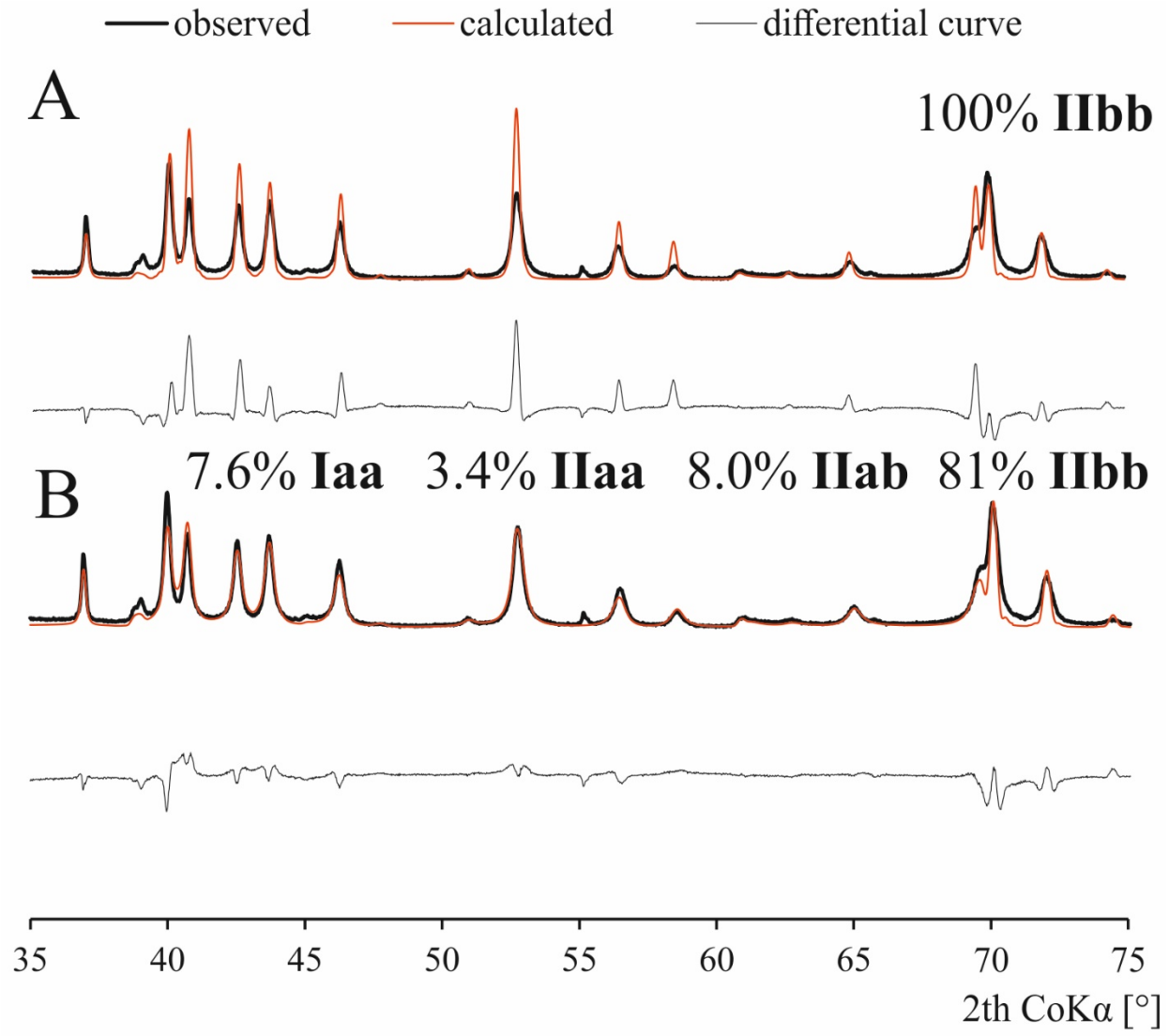

Figure SI 16. Comparison of fits for SG7 chlorite **A)** without and **B)** with consideration of interstratification with polytypes other than IIbb.

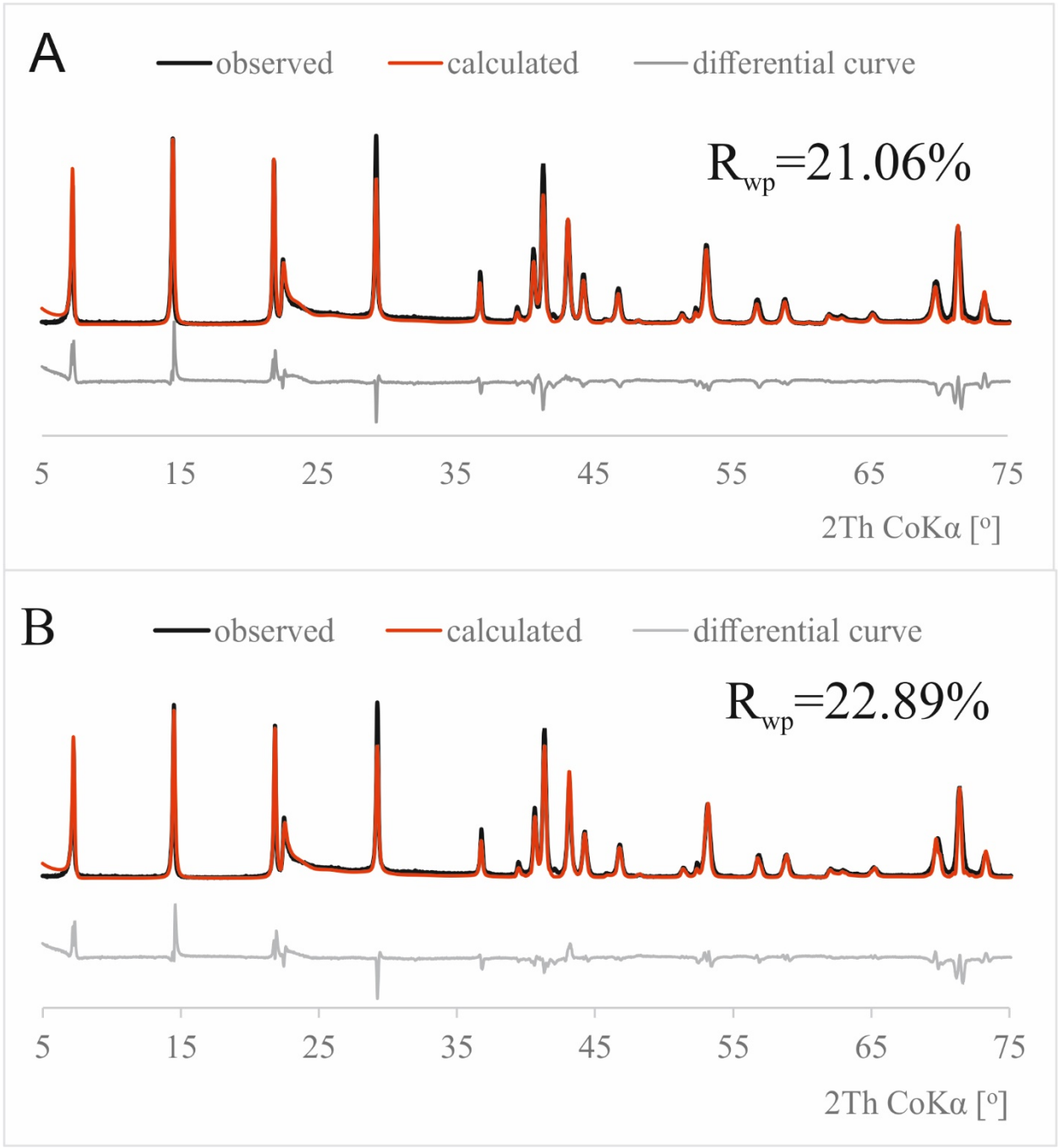

Figure SI 17. Comparison of fits for POST chlorite **A)** with assumed R0 ordering **B)** with assumed R1 ordering.

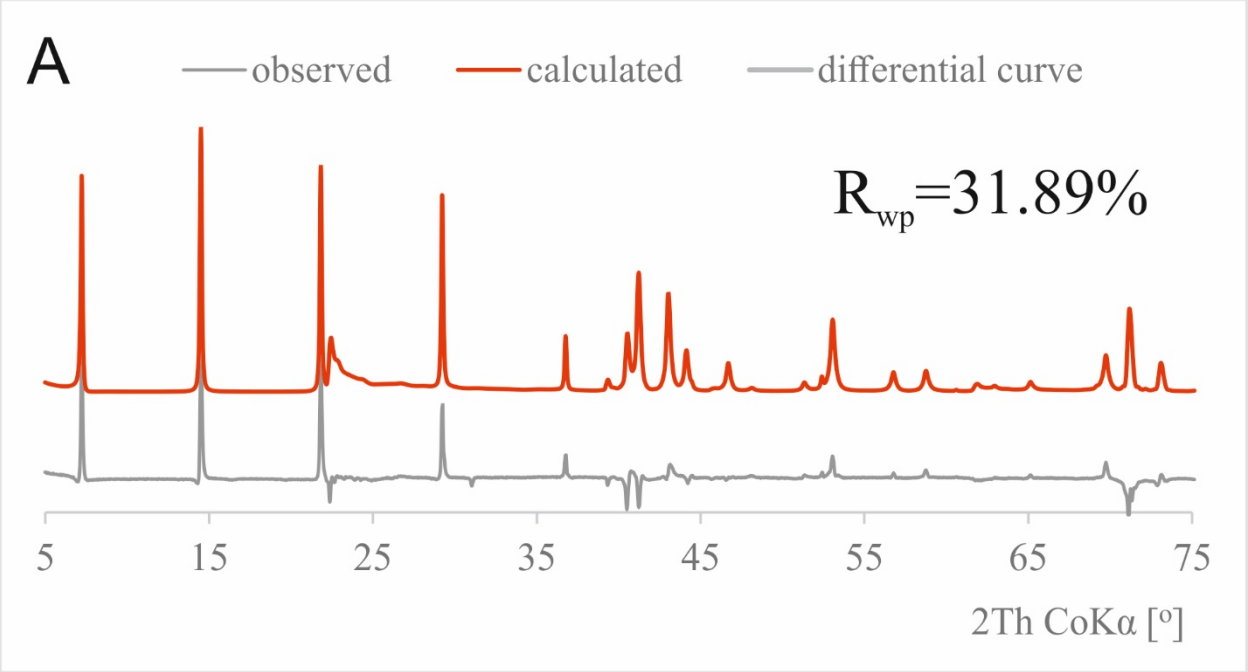

Figure SI 18 A. MAL chlorite with assumed R0 ordering.

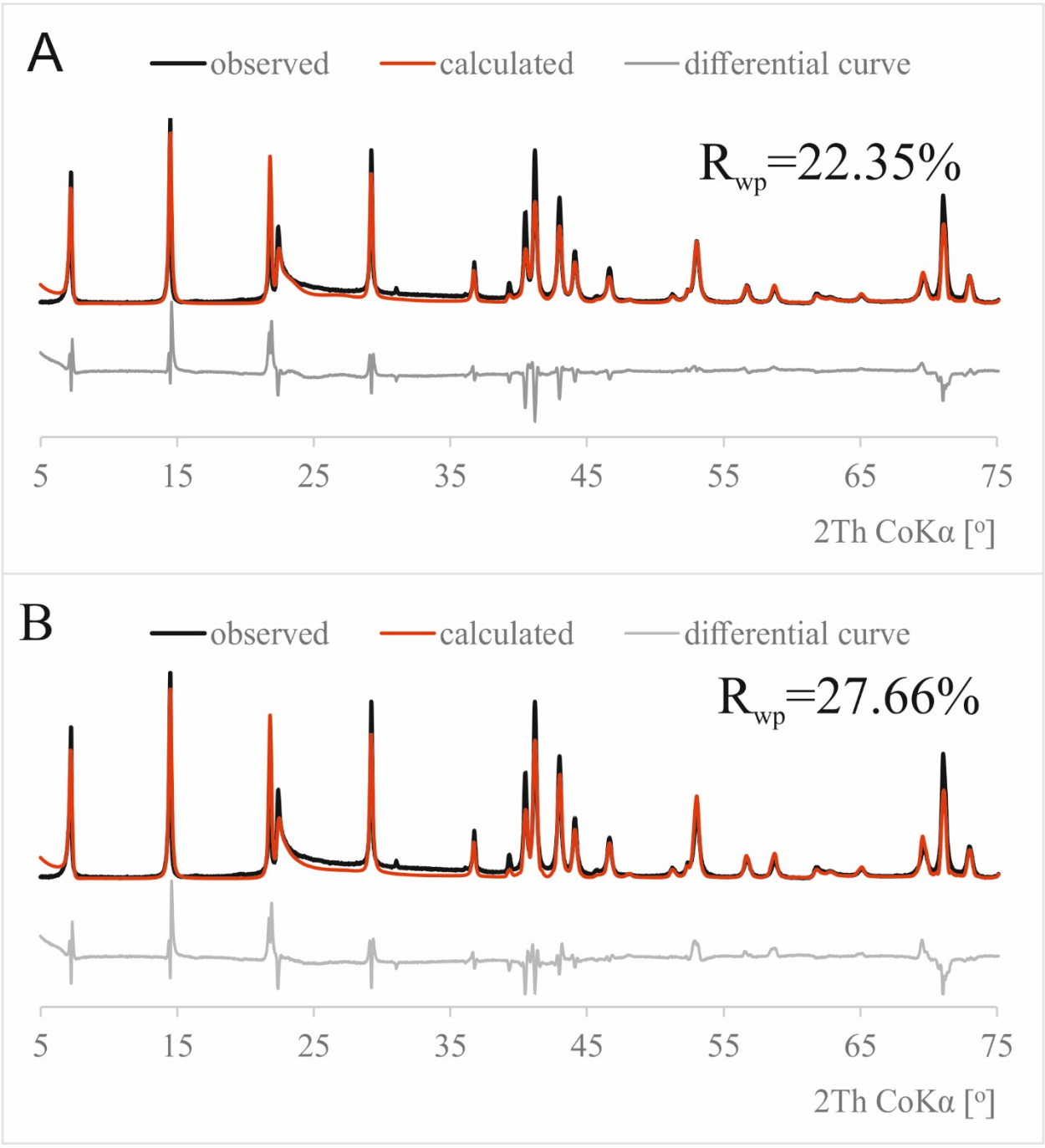

Figure SI 19. Comparison of fits for CCC chlorite **A)** with assumed R0 ordering **B)** with assumed R1 ordering.

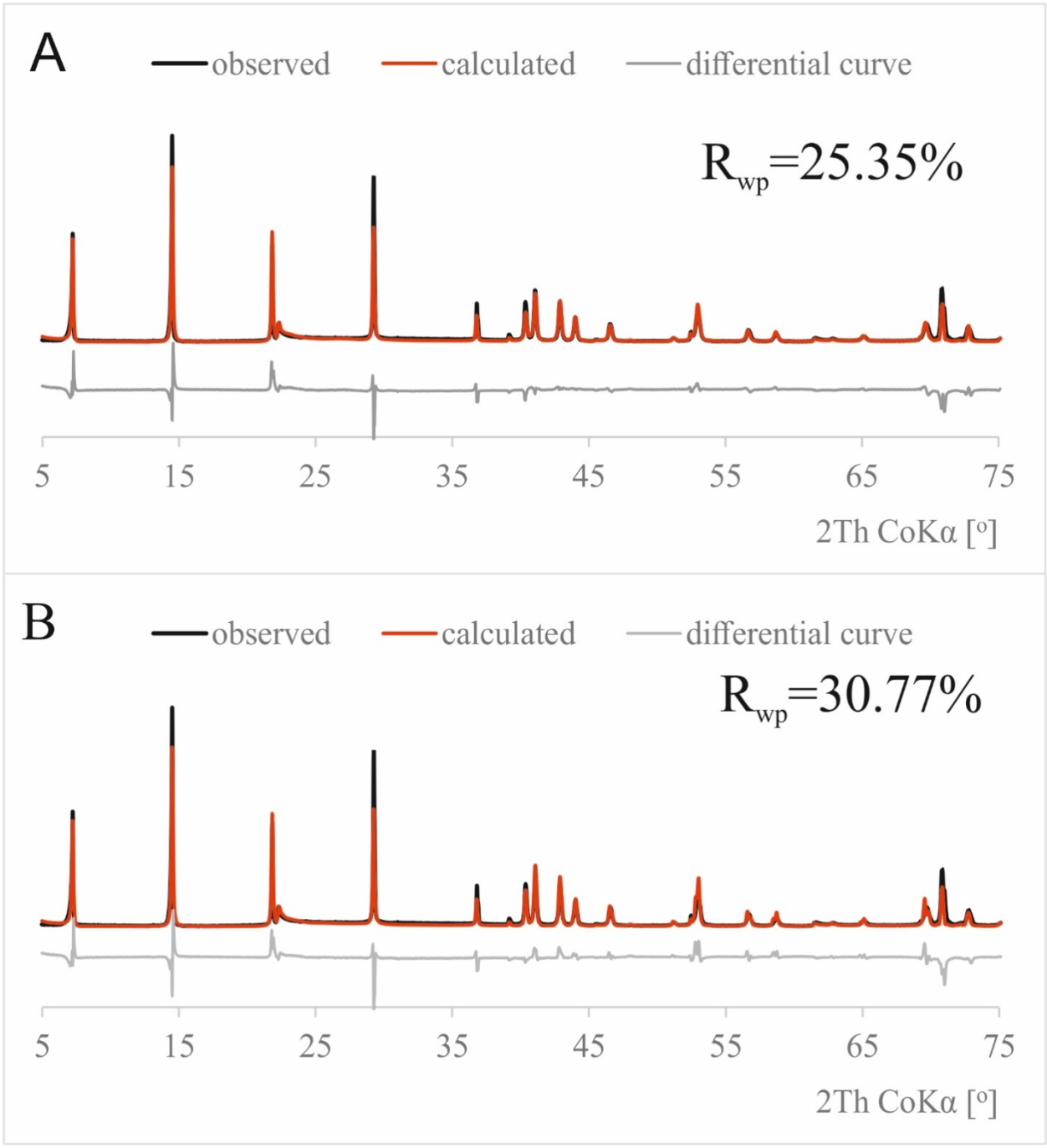

Figure SI 20. Comparison of fits for Sptb chlorite **A)** with assumed R0 ordering **B)** with assumed R1 ordering.

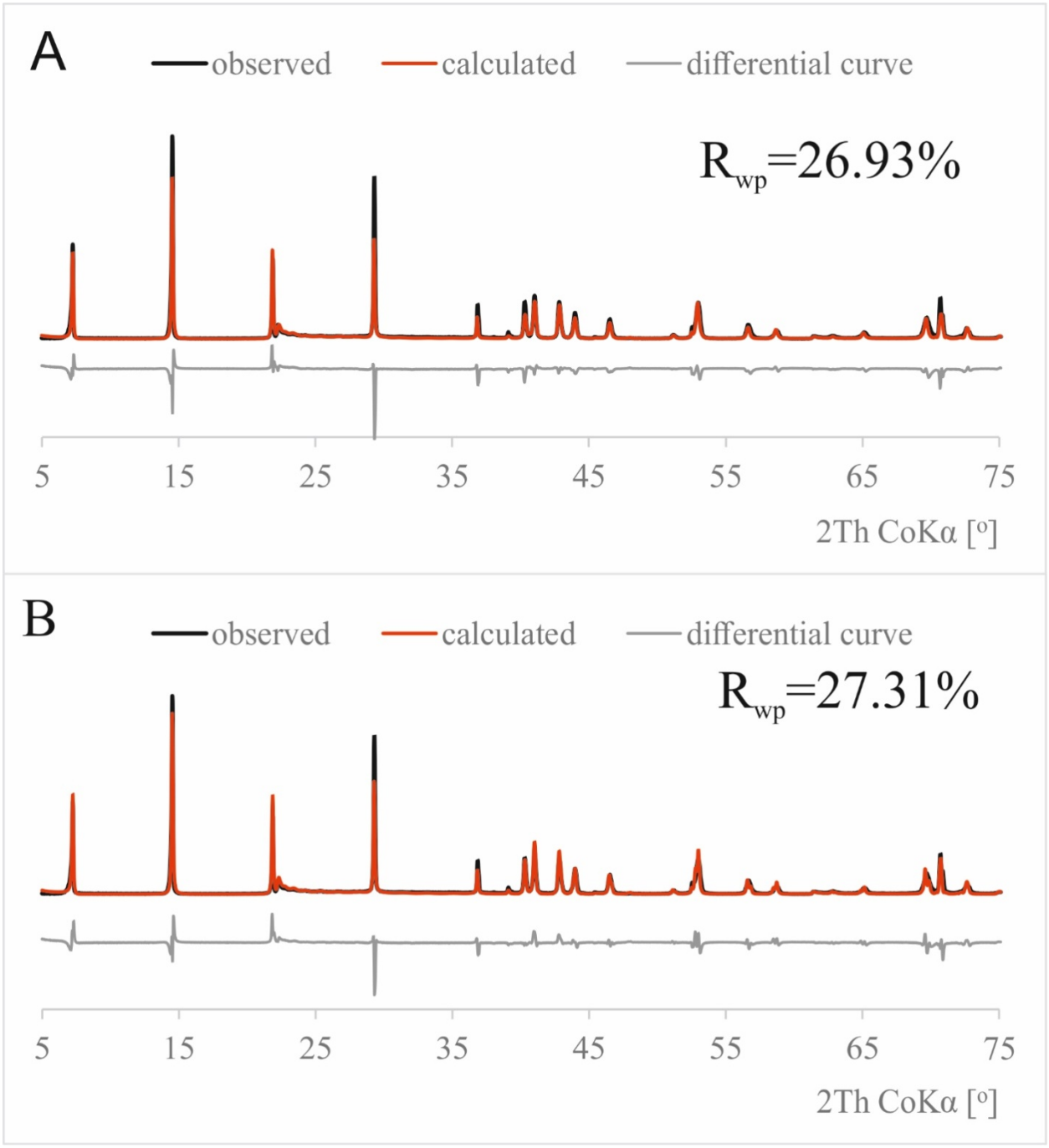

Figure SI 21. Comparison of fits for CCa-2 chlorite **A)** with assumed R0 ordering **B)** with assumed R1 ordering.

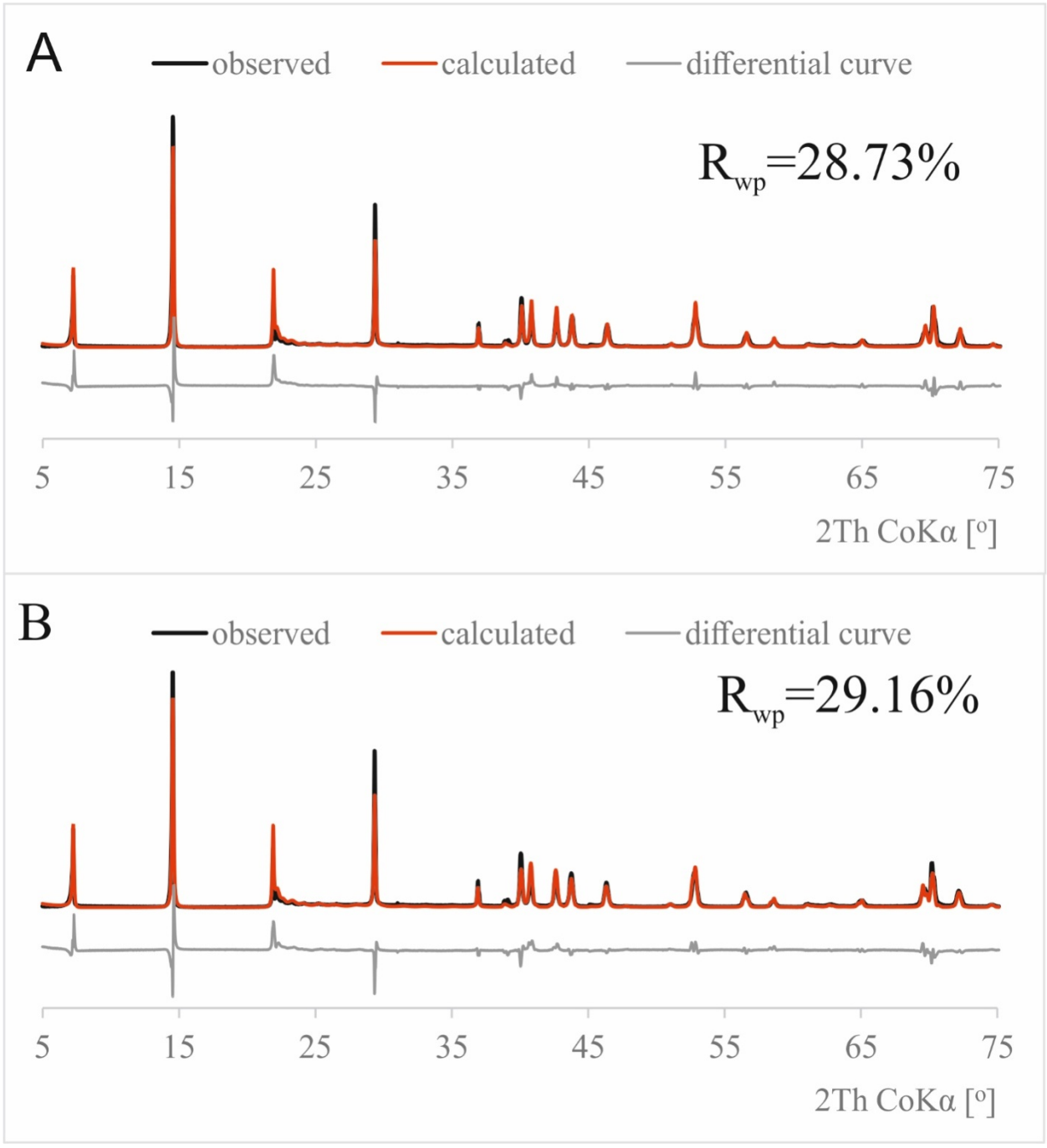

Figure SI 22. Comparison of fits for Mtbl chlorite **A)** with assumed R0 ordering **B)** with assumed R1 ordering.

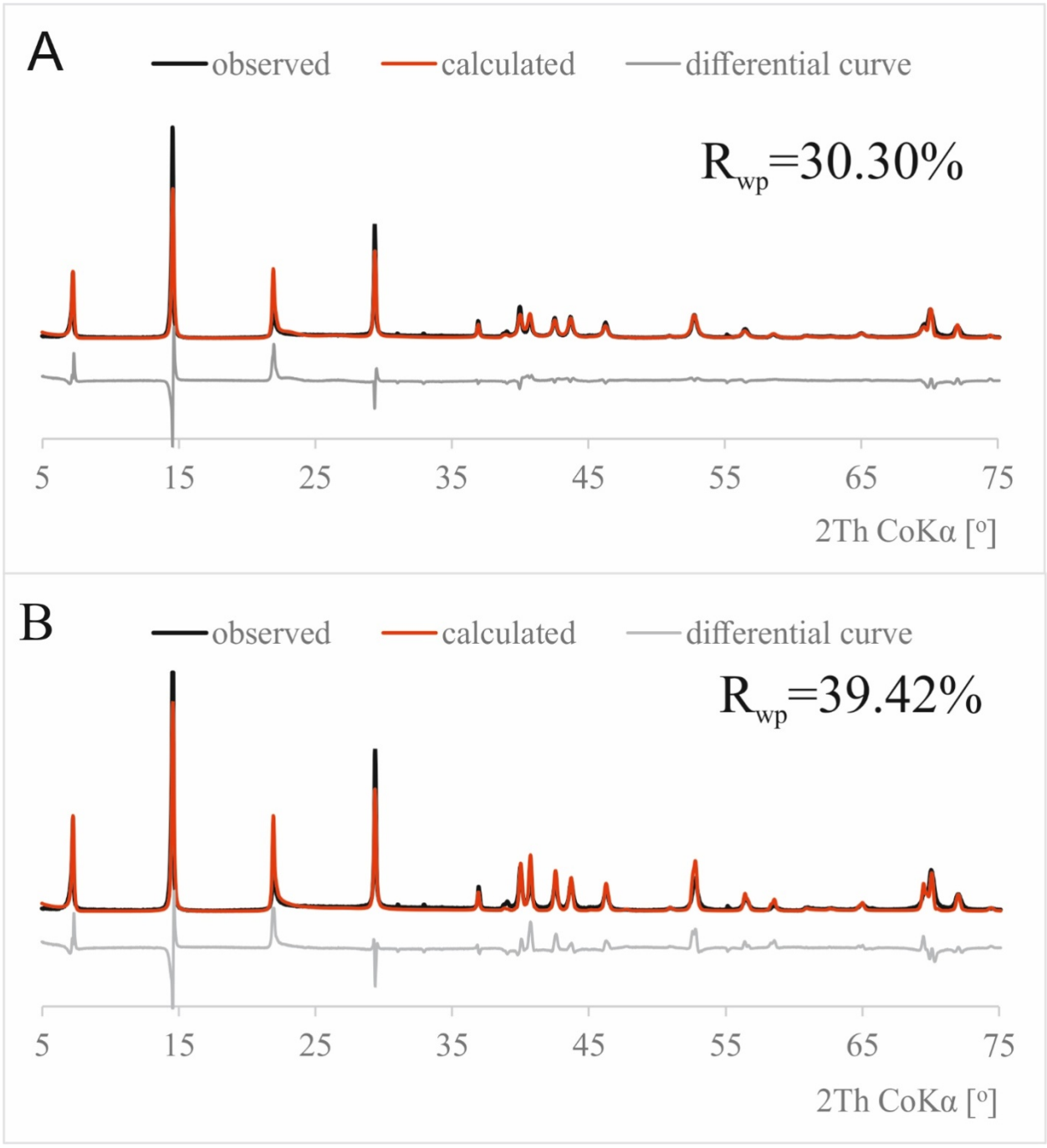

Figure SI 23. Comparison of fits for SG7 chlorite **A)** with assumed R0 ordering **B)** with assumed R1 ordering.

Analysis of possible disorder of orientation of 2:1 layersin 0°, 120° and 240°and shifts along **b** for successive 2:1 layers in IIbb polytype has been performed. The results show that there should be no difference between powder patterns within the following two groups:

(1) rot0, y=1/3**b**; rot0, y=-1/3**b**; rot120, y=0**b**; rot 120, y=-1/3**b**; rot240, y=0**b**; rot 240, y=+1/3 **b**

(2) rot0, y=0**b**; rot120, y=+1/3**b**; rot240, y=-1/3**b**

This is visible for powder patterns of each of these end-member structures. Equivalence for rot0, y=0**b** and rot120, y=+1/3**b** structures is shown in the following discussion. Similar analysis can be performed for all the pairs within these two groups.

Structural model of chlorite implemented in Sybilla 3D

In Sybilla 3D program, model of chlorite structure assumes orthogonal unit cell in which the beta angle ($\neq 90^{o}$) is manifested by layer shift parallel to **a**. In the case of IIbb chlorite this is achieved by value of -1/3**a**, which corresponds to angle beta of c.a. 97^{o} (Figure SI 24) depending on exact values of a and c, which are independently optimized. In the ab plane the chlorite structure assumes ditrigonal shape of cavity in the tetrahedral sheet (Figure SI 25). "Talc stagger" vector is defined as displacement from lower to upper basal oxygens of 2:1 layer (cf. Fig. 1 in Brown and Bailey, 1962).

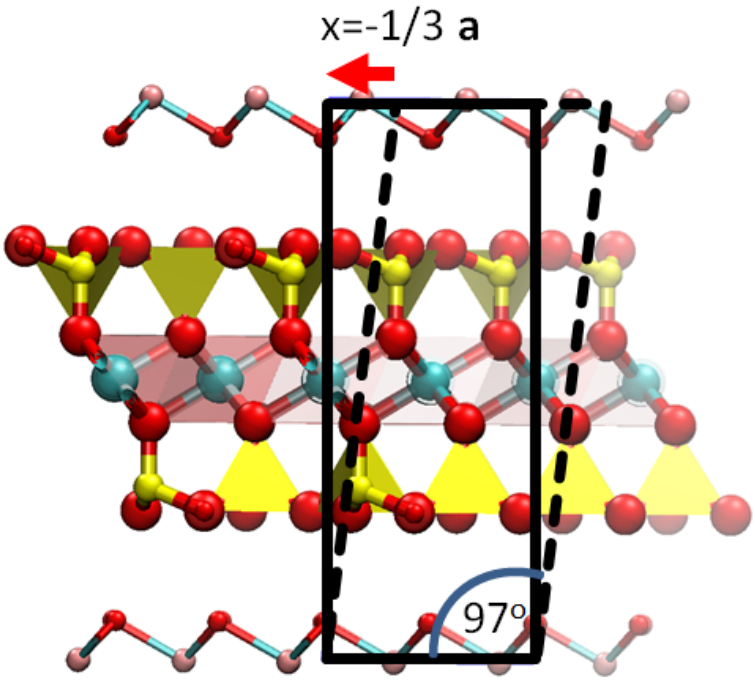

Figure SI 24. IIbb chlorite unit cell displayed in xz plane. Shift by -1/3**a** in consecutive unit cells is equivalent to beta angle of c.a. 97^{o}. Solid black line – chlorite unit cell implemented in Sybilla 3D. "Talc stagger" is marked with red arrow.

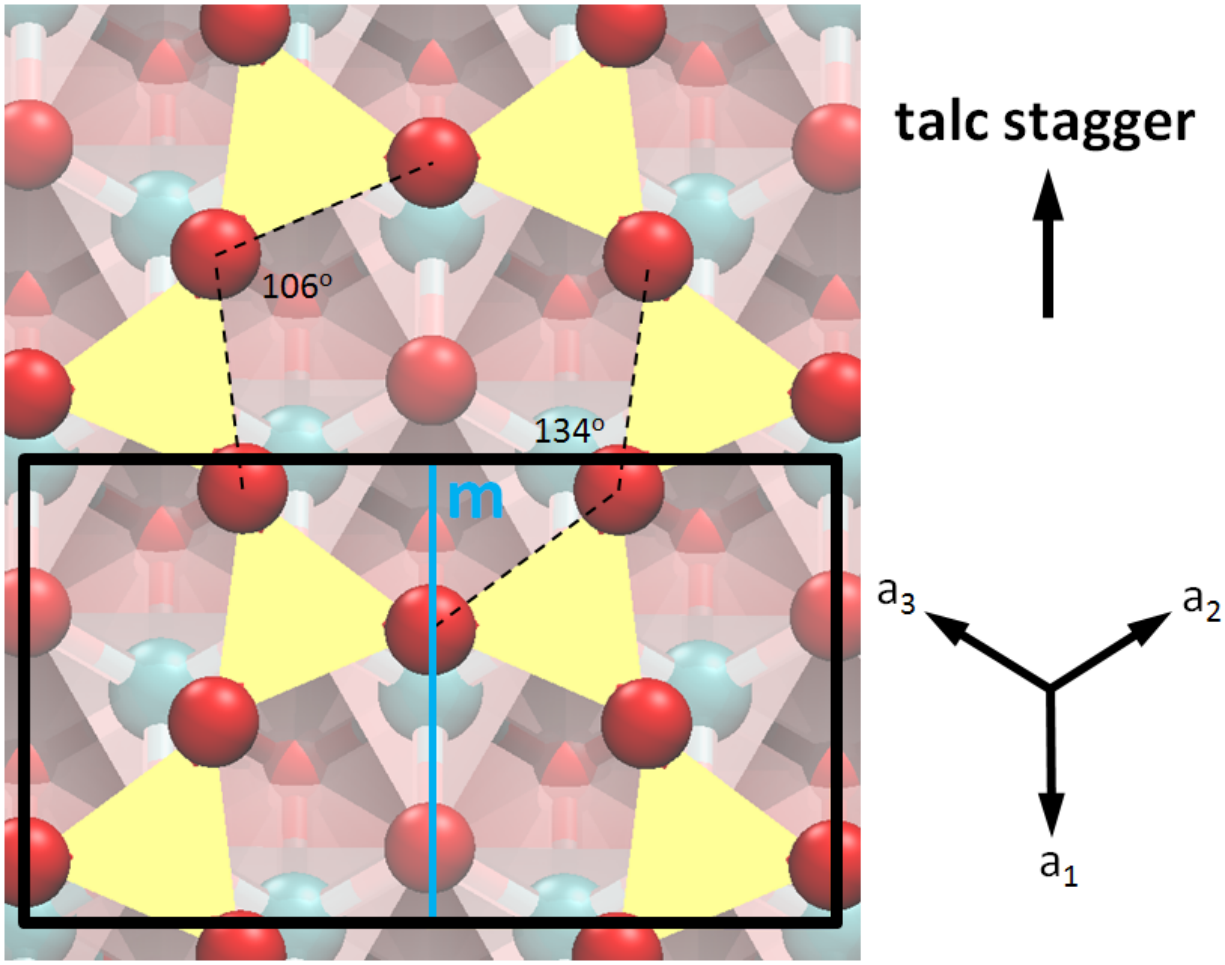

Figure SI 25. Structure of tetrahedral sheet of the studied chlorites with unit cell in the ab plane. Angles O-O-O are marked. All other atoms, except for basal oxygens, maintain hexagonal symmetry.Mirror plane is marked in blue.

Equivalence for rot0, y=0b and rot120, y=+1/3 b structures

In the case of structure rot0, y=0**b** each consecutive unit cell above the initial one is shifted by -1/3**a**. I the case of rot0, y=+1/3**b** the shifts are therefore: (-1/3**a**, 1/3**b**), which for third unit cell is equal to (**a**, **b**), i.e. final position in the ab plane is the same in the initial unit cell (Figure SI 26).

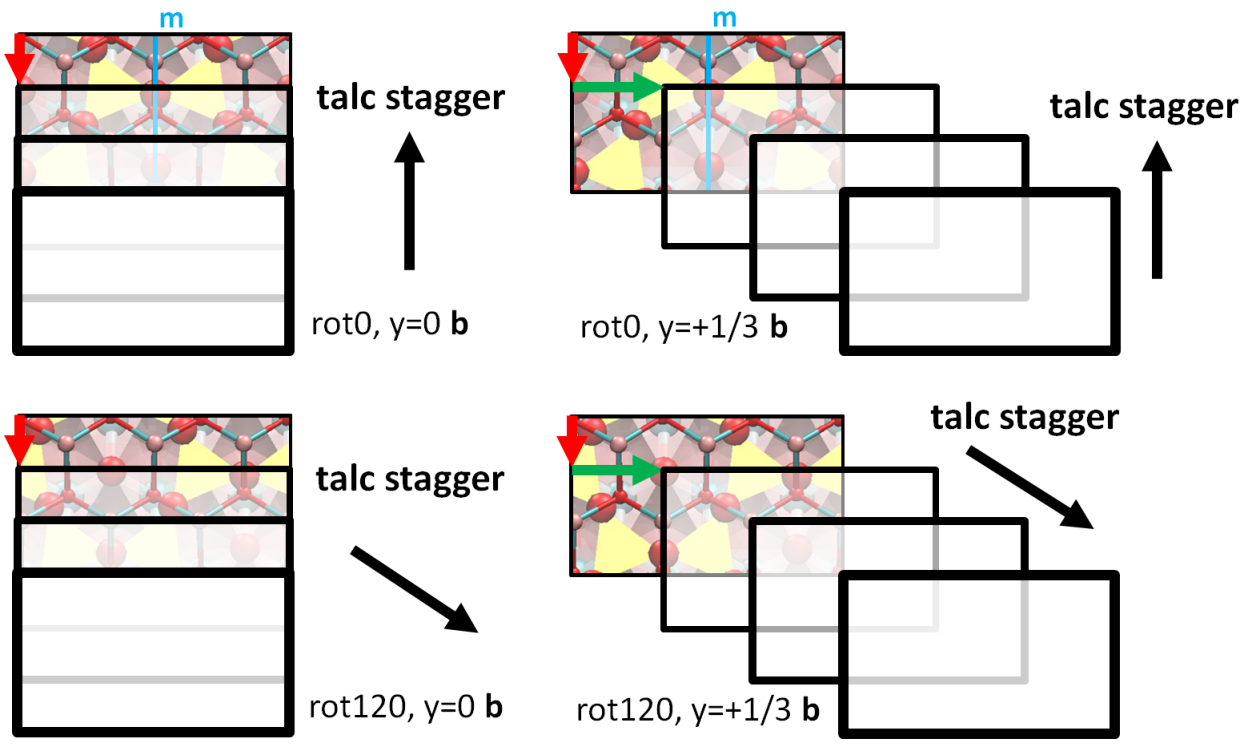

Figure SI 26. Structures with rot0 and rot120, with translations y=0**b** and y=1/3**b**. Shifts in **a** (-1/3**a**) are marked with red arrow, while shifts in **b** (1/3**b**) are marked with green one. "Talc stagger" direction marked with black arrow. For rot0 the lowest (initial) unit cell have mirror plane shown in Figure 2, which is not visible for rot120.

For structure with rot120, y= +1/3**b** it is possible to define new unit cell that is rotated by 120º (Figure SI 27) relatively to the initial one (Figure SI 26). The new unit cell have mirror plane and can be assumed that within the new (rotated) previously translated by -1/3**a** and 1/3**b** can be simplified to be equal to –**a**/3.

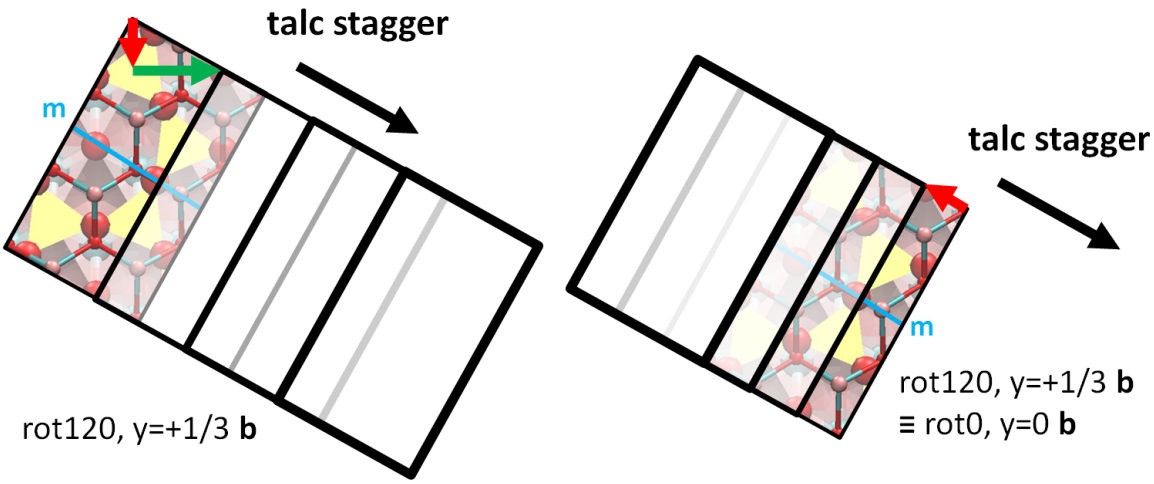

Figure SI 27. Structure with rot120, y= +1/3**b**, which is equivalent to rot0, y=0**b** when assuming orientation of unit cell by 120^{o}, that contains mirror plane (parallel to talc stagger).